Dynamical Thermalization in the Quark-Meson Model

with J. Berges, J. Pawlowski, A. Rothkopf

666. WE-Heraeus-Seminar
"From Correlation Functions to QCD Phenomenology"
April 3 - 6, 2018, Bad Honnef

From heavy ion collisions towards the QCD phase diagram: an equilibration process

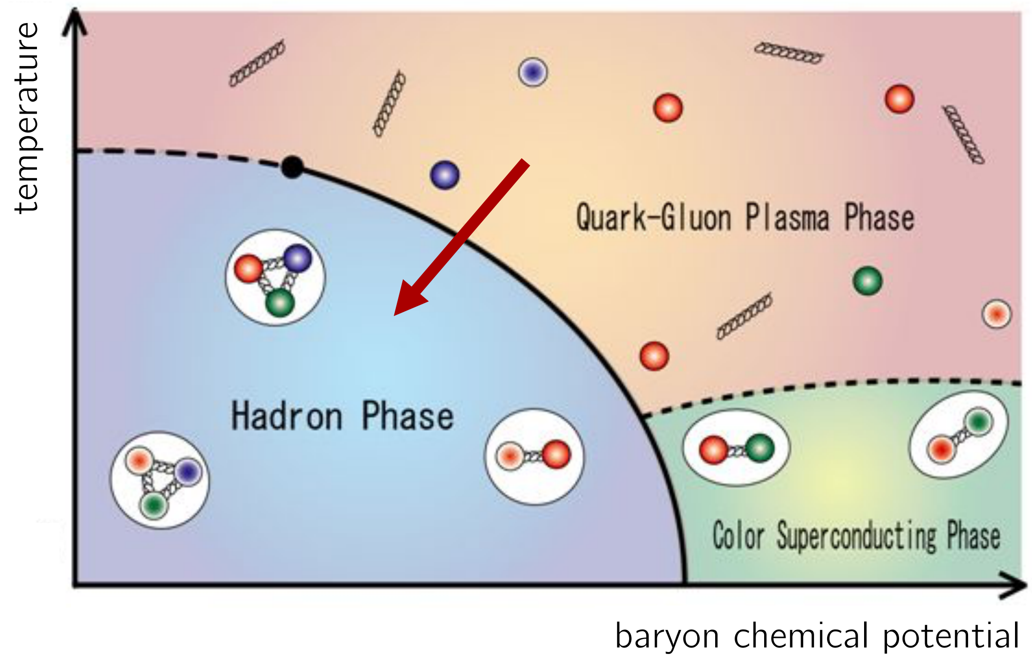

- QCD phase diagram: an equilibrium concept
- deconfinement + chiral phase transition

Figures from http://wl33.web.rice.edu/images/HI-cartoon.png, http://images.slideplayer.com/25/7893277/slides/slide_3.jpg

From heavy ion collisions towards the QCD phase diagram: an equilibration process

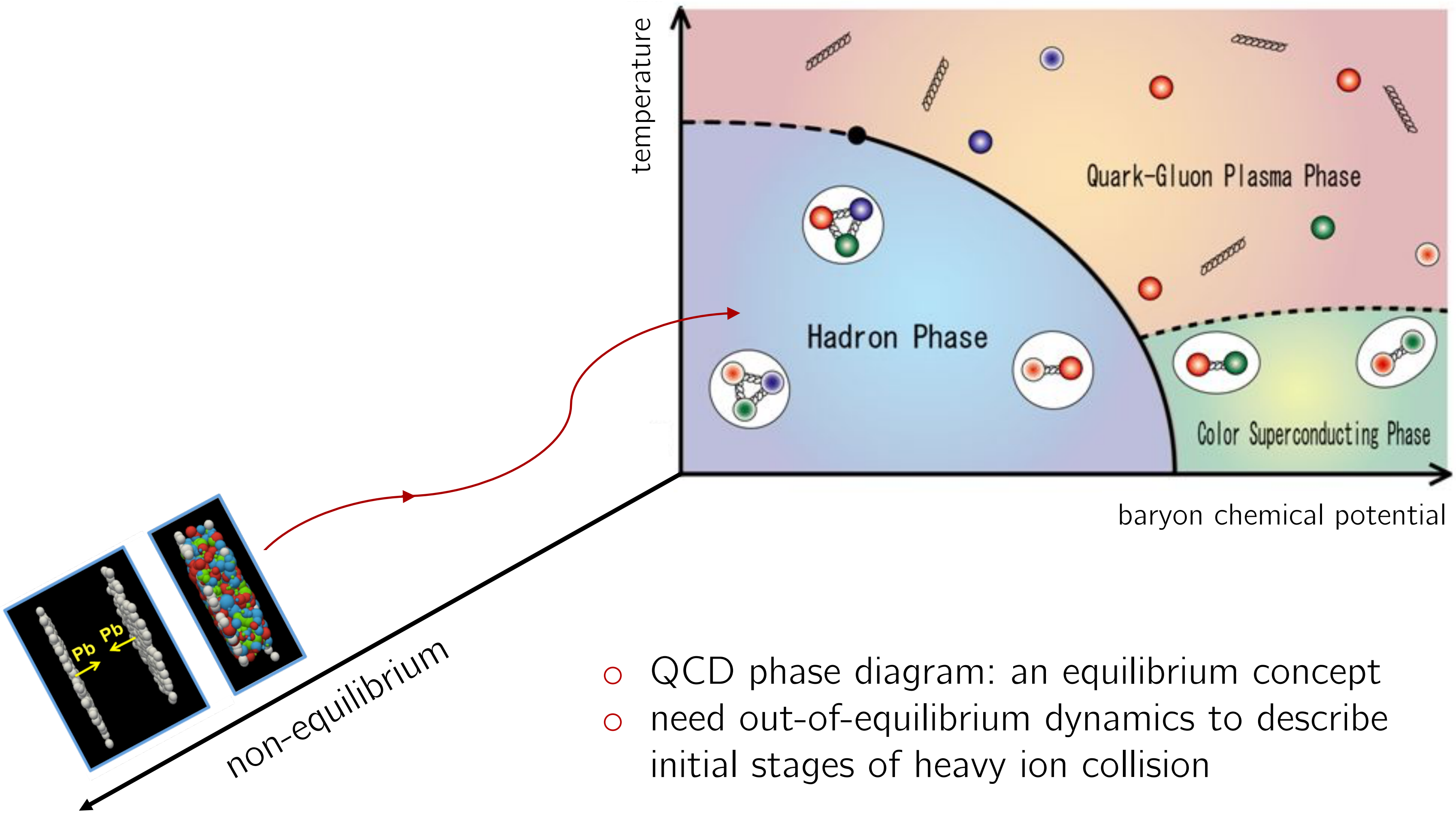

- QCD phase diagram: an equilibrium concept
- need out-of-equilibrium dynamics to describe initial stages of heavy ion collision

Figures from http://wl33.web.rice.edu/images/HI-cartoon.png, http://images.slideplayer.com/25/7893277/slides/slide_3.jpg

From heavy ion collisions towards the QCD phase diagram: an equilibration process

non-perturbative regime of QCD

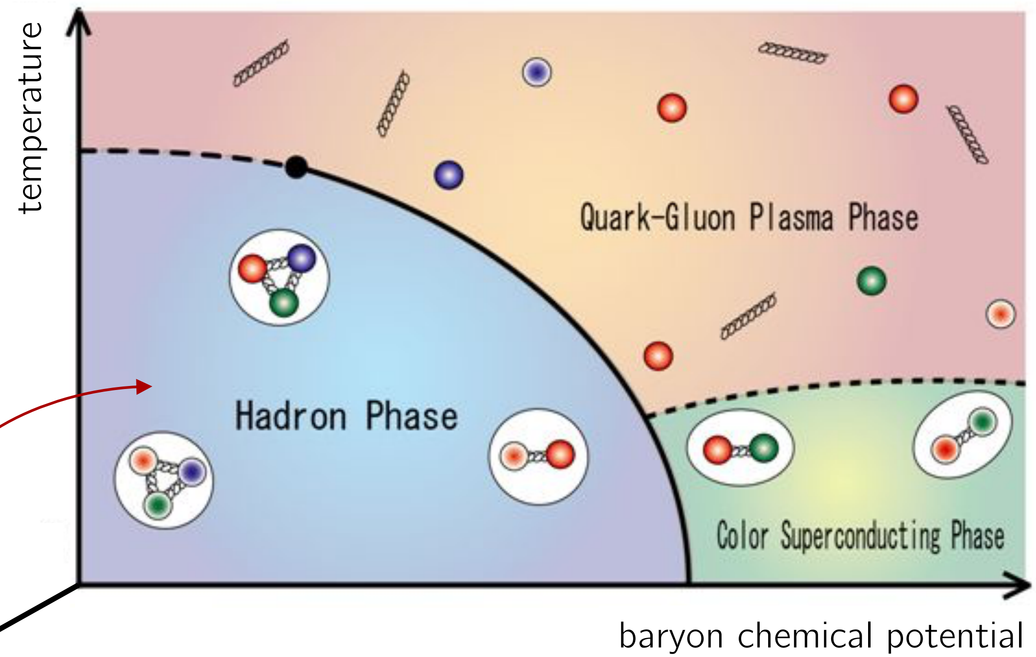

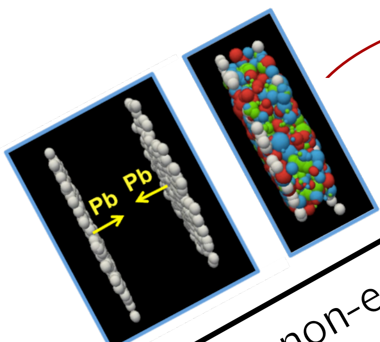

non-equilibrium

- QCD phase diagram: an equilibrium concept
- need out-of-equilibrium dynamics to describe initial stages of heavy ion collision

Figures from http://wl33.web.rice.edu/images/HI-cartoon.png, http://images.slideplayer.com/25/7893277/slides/slide_3.jpg

We can investigate this equilibration using effective field theories.

- low-energy QCD

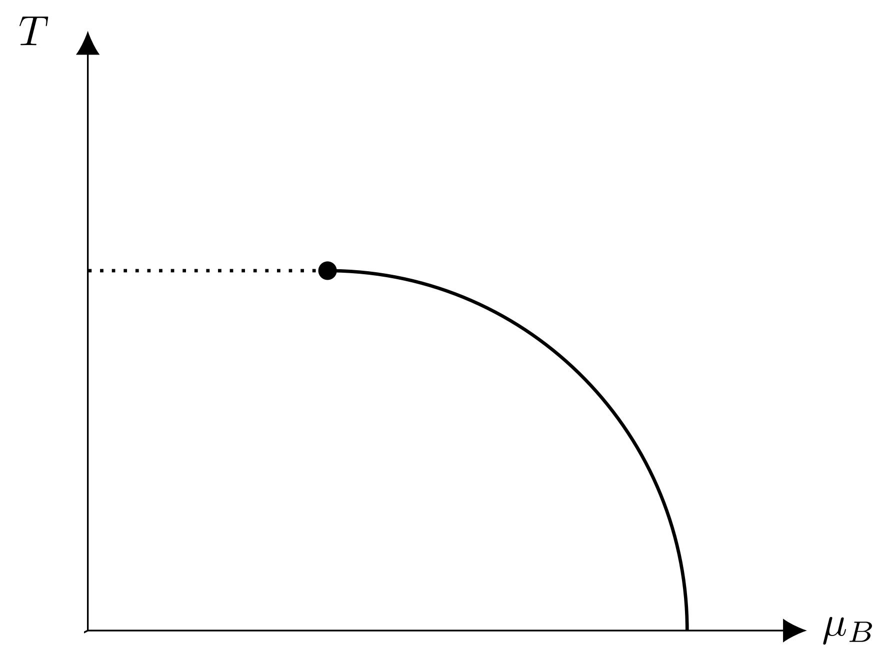

We can investigate this equilibration using effective field theories.

- low-energy QCD
- non-equilibrium dynamics

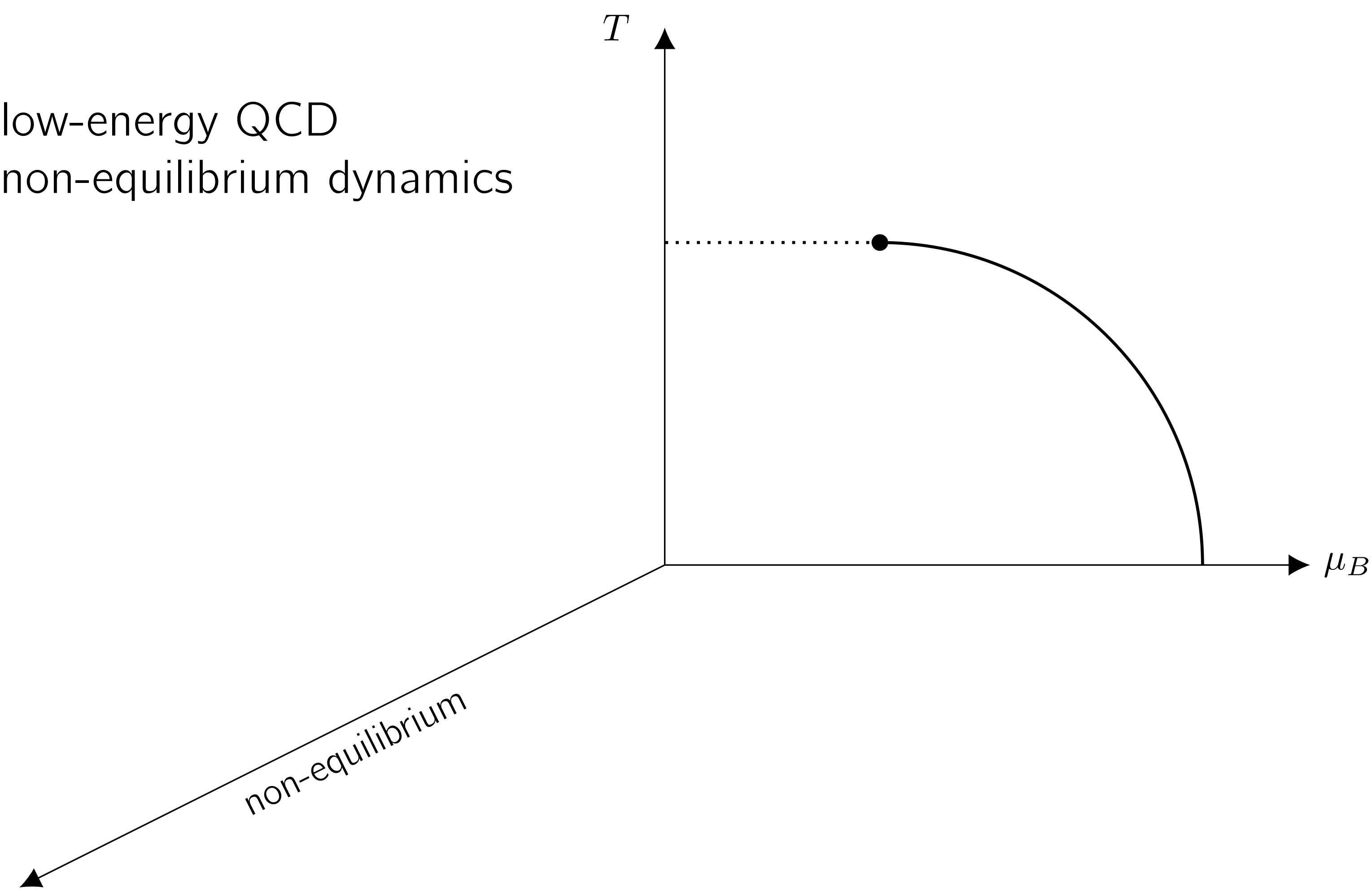

We can investigate this equilibration using effective field theories.

- low-energy QCD
- non-equilibrium dynamics
- approach of thermal state

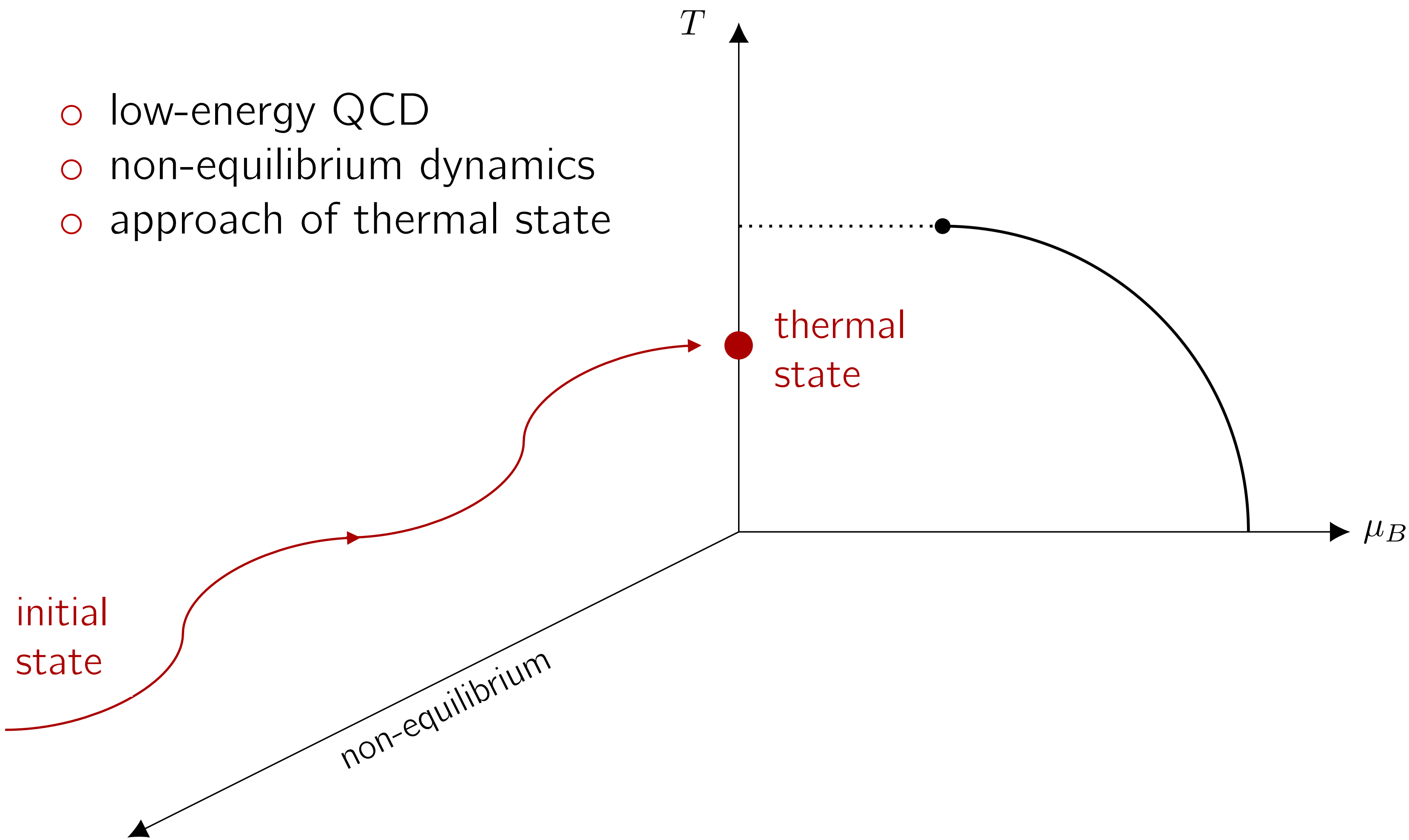

We can investigate this equilibration using effective field theories.

1. low-energy QCD
2. non-equilibrium dynamics
3. approach of thermal state

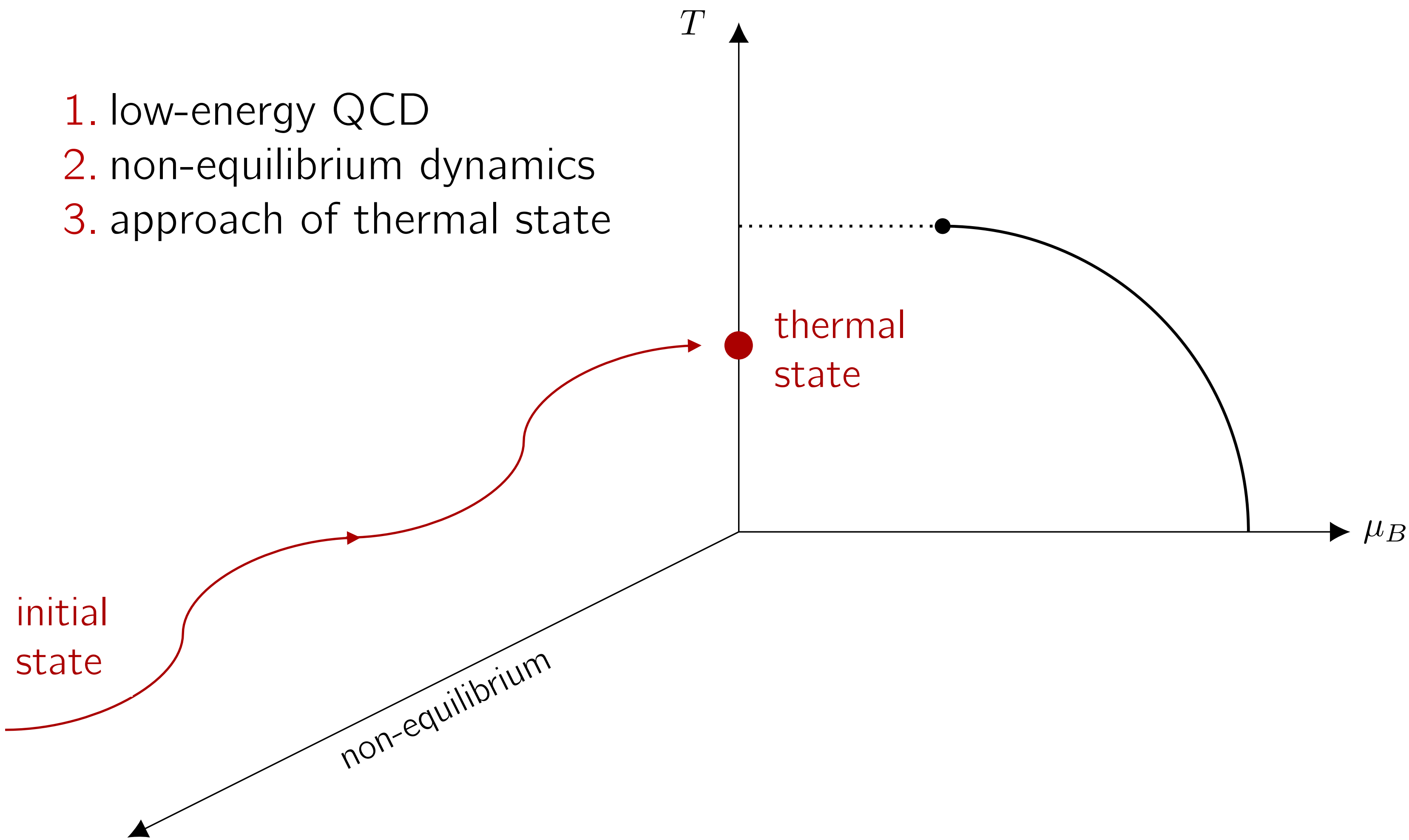

The quark-meson model provides a successful formulation of QCD below scales ~1 GeV.

- d.o.f.: light quarks and mesons
- chiral symmetry breaking
- phase diagram with 1st order & 2nd order/crossover transition

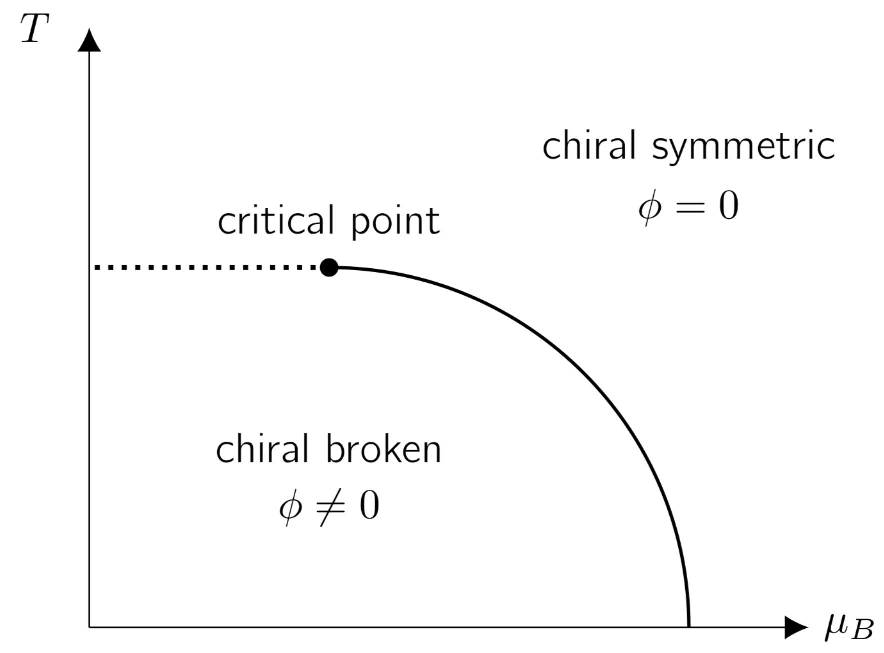

Jungnickel, Wetterich. PRD (1996)
Birse. J. Phys. G: Nucl. Part. Phys. (1994)
Petropoulos. J. Phys. G: Nucl.Part. Phys (1998)
Berges, Jungnickel, Wetterich.Int. J. Mod. Phys. A (2003)
Schaefer, Pirner. arXiv nucl-th/9903003 (1999)

The quark-meson model provides a successful formulation of QCD below scales ~1 GeV.

- d.o.f.: light quarks and mesons
- chiral symmetry breaking
- phase diagram with 1st order & 2nd order/crossover transition

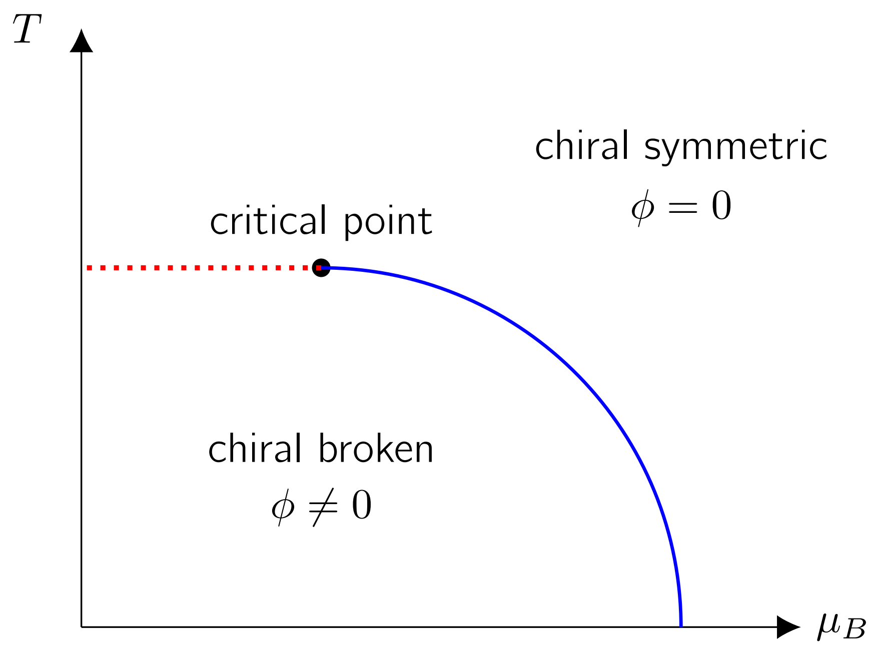

Jungnickel, Wetterich. PRD (1996)
Birse. J. Phys. G: Nucl. Part. Phys. (1994)
Petropoulos. J. Phys. G: Nucl.Part. Phys (1998)
Berges, Jungnickel, Wetterich.Int. J. Mod. Phys. A (2003)
Schaefer, Pirner. arXiv nucl-th/9903003 (1999)

The quark-meson model provides a successful formulation of QCD below scales ~1 GeV.

$$S[\bar{\psi}, \psi, \sigma, \pi] = \int_x \Bigg[\bar{\psi}\left[i\gamma^\mu \partial_\mu - m_\psi\right]\psi - \frac{g}{N_f}\bar{\psi}\left[\sigma + i\gamma_5 \tau^\alpha \pi^\alpha\right]\psi + \frac{1}{2}\left[\partial_\mu \sigma \partial^\mu \sigma + \partial_\mu \pi \partial^\mu \pi\right] - \frac{1}{2}m^2\left[\sigma^2 + \pi^\alpha \pi^\alpha\right] - \frac{\lambda}{4! N}\left[\sigma^2 + \pi^\alpha \pi^\alpha\right]^2 \Bigg]$$

The quark-meson model provides a successful formulation of QCD below scales ~1 GeV.

u & d quark

$$S[\bar{\psi}, \psi, \sigma, \pi] = \int_x \Big[\bar{\psi} \left[i\gamma^\mu \partial_\mu - m_\psi \right] \psi - \frac{g}{N_f} \bar{\psi} \left[\sigma + i\gamma_5 \tau^\alpha \pi^\alpha \right] \psi + \frac{1}{2} \left[\partial_\mu \sigma \partial^\mu \sigma + \partial_\mu \pi \partial^\mu \pi \right] - \frac{1}{2} m^2 \left[\sigma^2 + \pi^\alpha \pi^\alpha \right] - \frac{\lambda}{4! N} \left[\sigma^2 + \pi^\alpha \pi^\alpha \right]^2 \Big]$$

The quark-meson model provides a successful formulation of QCD below scales ~1 GeV.

u & d quark

$$S[\bar{\psi}, \psi, \sigma, \pi] = \int_x \Bigg[\bar{\psi}\left[i\gamma^\mu \partial_\mu - m_\psi\right]\psi - \frac{g}{N_f}\bar{\psi}\left[\sigma + i\gamma_5\tau^\alpha\pi^\alpha\right]\psi + \frac{1}{2}\left[\partial_\mu\sigma\partial^\mu\sigma + \partial_\mu\pi\partial^\mu\pi\right] - \frac{1}{2}m^2\left[\sigma^2 + \pi^\alpha\pi^\alpha\right] - \frac{\lambda}{4!N}\left[\sigma^2 + \pi^\alpha\pi^\alpha\right]^2 \Bigg]$$

sigma meson & pions

The quark-meson model provides a successful formulation of QCD below scales ~1 GeV.

u & d quark

Yukawa coupling

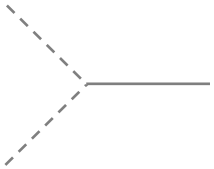

$$S[\bar{\psi}, \psi, \sigma, \pi] = \int_x \Big[\bar{\psi}\left[i\gamma^\mu \partial_\mu - m_\psi\right]\psi - \frac{g}{N_f}\bar{\psi}\left[\sigma + i\gamma_5 \tau^\alpha \pi^\alpha\right]\psi$$

$$+ \frac{1}{2}\left[\partial_\mu \sigma \partial^\mu \sigma + \partial_\mu \pi \partial^\mu \pi\right] - \frac{1}{2} m^2 \left[\sigma^2 + \pi^\alpha \pi^\alpha\right] - \frac{\lambda}{4! N}\left[\sigma^2 + \pi^\alpha \pi^\alpha\right]^2 \Big]$$

sigma meson & pions

The quark-meson model provides a successful formulation of QCD below scales ~1 GeV.

u & d quark   Yukawa coupling

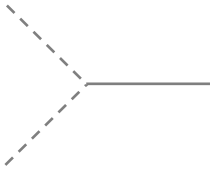

$$S[\bar{\psi},\psi,\sigma,\pi] = \int_x \Big[\, \bar{\psi}\,[i\gamma^\mu\partial_\mu - m_\psi]\,\psi - \frac{g}{N_f}\bar{\psi}\,[\sigma + i\gamma_5\tau^\alpha\pi^\alpha]\,\psi + \frac{1}{2}\,[\partial_\mu\sigma\partial^\mu\sigma + \partial_\mu\pi\partial^\mu\pi] - \frac{1}{2}m^2\,[\sigma^2+\pi^\alpha\pi^\alpha] - \frac{\lambda}{4!N}\,[\sigma^2+\pi^\alpha\pi^\alpha]^2 \Big]$$

sigma meson & pions   scalar potential

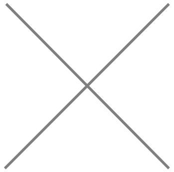

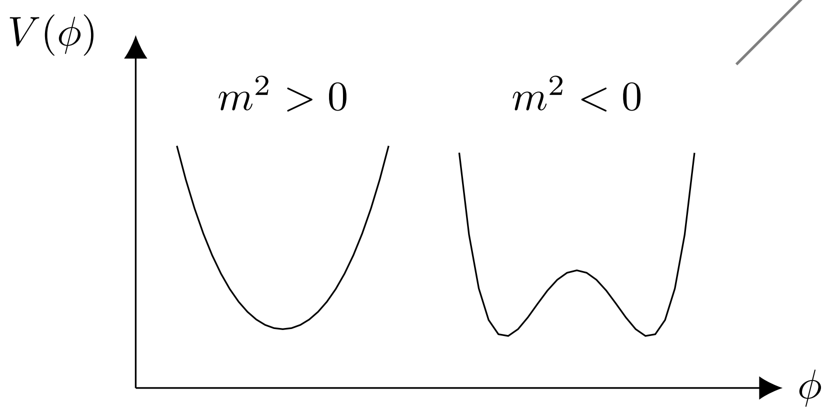

The 2PI effective action is a practical tool to study thermalization.

Berges. AIP Conference Proc. (2004)
Borsányi. arXiv hep-ph/0512308 (2005)

classical action
$S[\bar{\psi}, \psi, \sigma, \pi]$

↓

2PI effective action
$\Gamma[\phi, G]$

↓

evolution equations
for ϕ and G

The 2PI effective action is a practical tool to study thermalization.

Berges. AIP Conference Proc. (2004)
Borsányi. arXiv hep-ph/0512308 (2005)

classical action
$S[\bar{\psi}, \psi, \sigma, \pi]$

$\downarrow$

non-equilibrium

2PI effective action
$\Gamma[\phi, G]$

$\downarrow$

non-equilibrium

evolution equations
for ϕ and G

The 2PI effective action is a practical tool to study thermalization.

Berges. AIP Conference Proc. (2004)
Borsányi. arXiv hep-ph/0512308 (2005)

classical action
$S[\bar{\psi}, \psi, \sigma, \pi]$

$\downarrow$

non-equilibrium | 2PI effective action $\Gamma[\phi, G]$ | ✓ non-perturbative approximations

$\downarrow$

non-equilibrium | evolution equations for ϕ and G | ✓ non-secular and universal

classical action
$S[\bar{\psi}, \psi, \sigma, \pi]$

double Legendre transf.

2PI effective action
$\Gamma[\phi, G]$

evolution equations
for ϕ and G

non-equilibrium generating functional for $\rho^{\text{Gauss}}(t_0)$

$$Z[J,R] = e^{iW[J,R]} = \int \mathcal{D}\varphi \; e^{iS[\varphi] + iJ\cdot\varphi + \frac{i}{2}\varphi\cdot R\cdot\varphi}$$

with

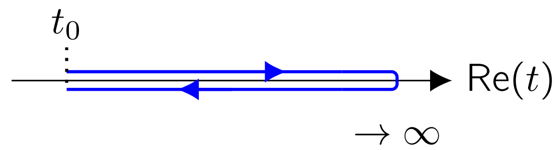

classical action
$S[\bar{\psi}, \psi, \sigma, \pi]$

non-equilibrium generating functional for $\rho^{\text{Gauss}}(t_0)$

$$Z[J,R] = e^{iW[J,R]} = \int \mathcal{D}\varphi \; e^{iS[\varphi] + iJ\cdot\varphi + \frac{i}{2}\varphi\cdot R\cdot\varphi}$$

with 

double
Legendre
transf.

2PI effective action
$\Gamma[\phi, G]$

$= S[\phi] +$ 1-loop quantum corrections $+$ 2PI diagrams

stationary
conditions

evolution equations
for ϕ and G

classical action
$S[\bar{\psi}, \psi, \sigma, \pi]$

double Legendre transf.

non-equilibrium generating functional for $\rho^{\text{Gauss}}(t_0)$

$$Z[J,R] = e^{iW[J,R]} = \int \mathcal{D}\varphi \; e^{iS[\varphi] + iJ\cdot\varphi + \frac{i}{2}\varphi\cdot R\cdot\varphi}$$

with

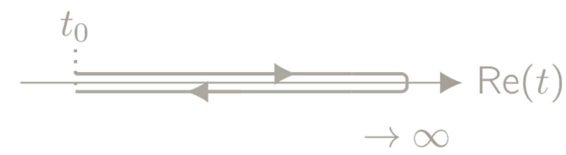

2PI effective action
$\Gamma[\phi, G]$

$= S[\phi] +$ 1-loop quantum corrections $+$ 2PI diagrams

large N expansion

$$\underbrace{\text{LO diagrams}}_{\sim N^1} + \underbrace{\text{NLO diagrams}}_{\sim N^0} + \;\dots\; + \text{fermion-boson-loop}$$

stationary conditions

evolution equations for ϕ and G

classical action
$S[\bar\psi, \psi, \sigma, \pi]$

non-equilibrium generating functional for $\rho^{\text{Gauss}}(t_0)$

$$Z[J,R] = e^{iW[J,R]} = \int \mathcal{D}\varphi \; e^{iS[\varphi] + iJ\cdot\varphi + \frac{i}{2}\varphi\cdot R\cdot\varphi}$$

with

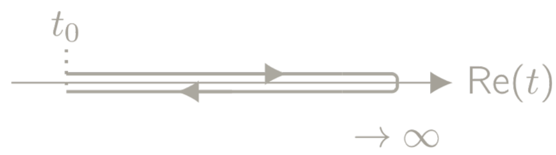

double
Legendre
transf.

2PI effective action
$\Gamma[\phi, G]$

$= S[\phi] +$ 1-loop quantum corrections $+$ 2PI diagrams

large N expansion

$$\underbrace{\text{LO diagrams}}_{\sim N^1} + \underbrace{\text{NLO diagrams}}_{\sim N^0} + \ \ldots\ + \text{fermion-boson-loop}$$

stationary
conditions

evolution equations
for ϕ and G

$$\left[\partial_t^2 + M^2(x;\phi)\right]\phi(t) = \text{fermion backreaction + 2PI corrections}$$

$$[\Box_x + M^2(x;\phi)]\,G(x,y) = -i\int_z [\Sigma(x,z;\phi,G)]\,G(z,y) - i\delta(x-y)$$

effective mass self-energy

Numerical solution of the equations of motion

- symmetries: spatial homogeneity & isotropy

- propagator decomposition:

$$G(x,y) = \underbrace{F(x,y)}_{\text{statistical function}} + \frac{i}{2}\underbrace{\rho(x,y)}_{\text{spectral function}}\ \mathsf{sgn}(x^0 - y^0)$$

- iterative real-time evolution

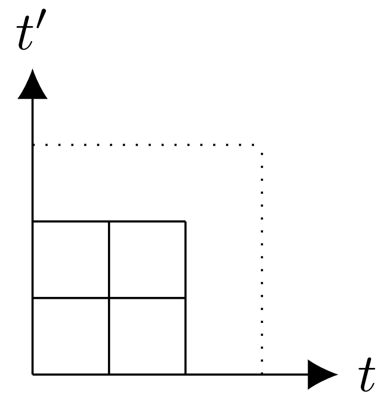

Numerical solution of the equations of motion

- symmetries: spatial homogeneity & isotropy

- propagator decomposition:

$$G(x,y) = \underbrace{F(x,y)}_{\text{statistical function}} + \frac{i}{2}\underbrace{\rho(x,y)}_{\text{spectral function}}\,\mathrm{sgn}(x^0 - y^0)$$

- iterative real-time evolution

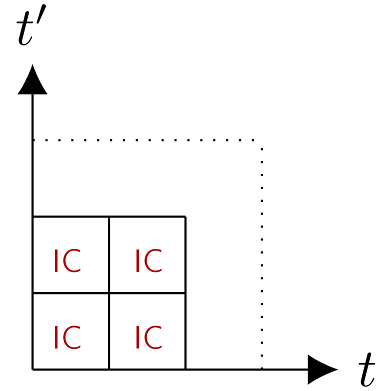

Numerical solution of the equations of motion

- symmetries: spatial homogeneity & isotropy

- propagator decomposition:

$$G(x,y) = F(x,y) + \frac{i}{2}\rho(x,y)\ \mathrm{sgn}(x^0 - y^0)$$

statistical function   spectral function

- iterative real-time evolution

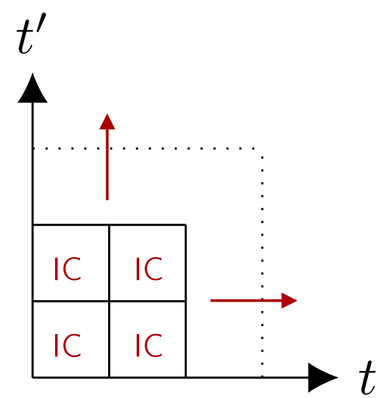

Real-time evolution of the macroscopic field

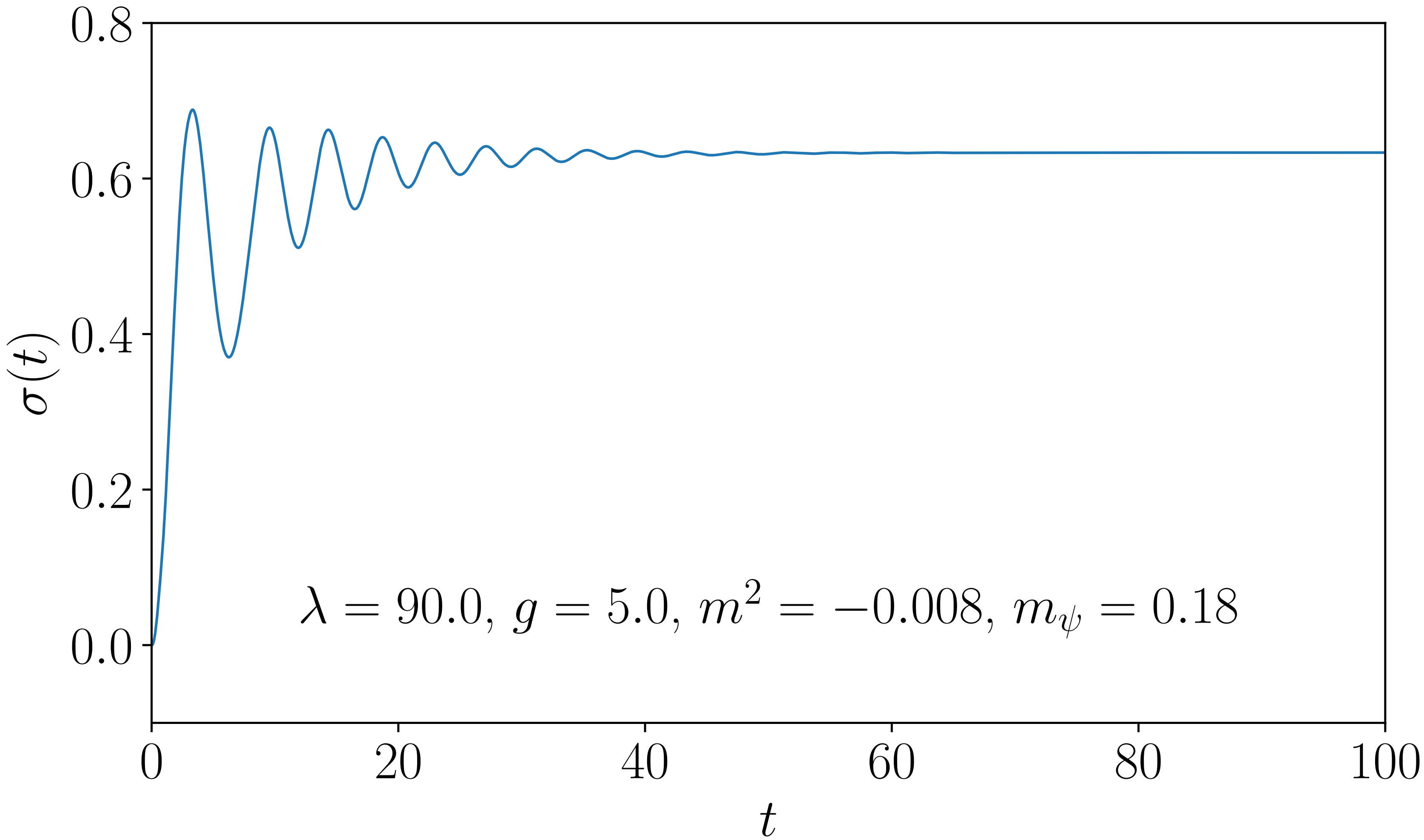

Real-time evolution of the macroscopic field

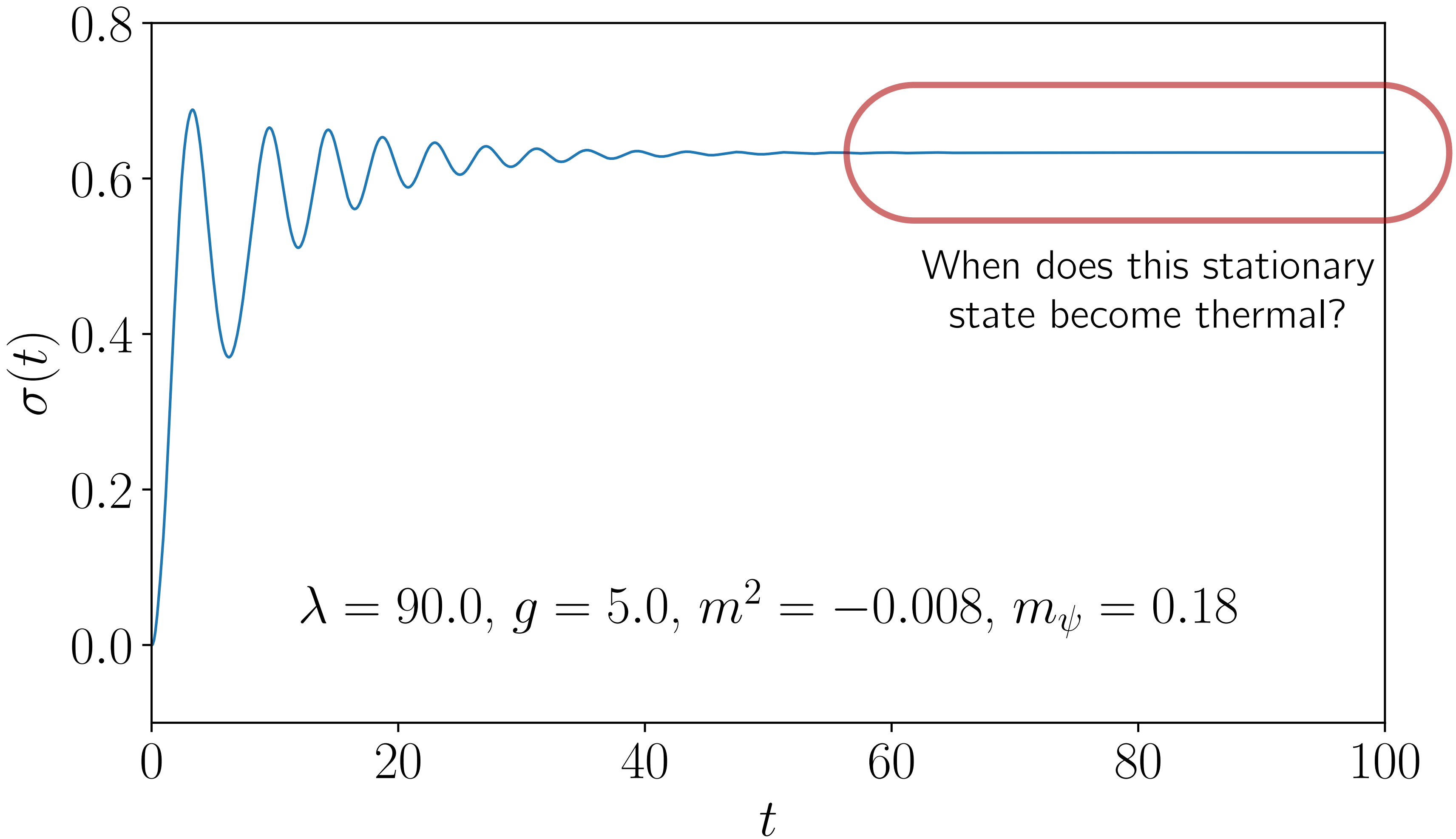

(1) Thermal equilibrium is a time-translation invariant state.

- time-translation invariance implies

$$G(t, t', |\mathbf{p}|) \rightsquigarrow G(\omega, |\mathbf{p}|)$$

in general depending on $t+t'$ and $t-t'$

independent of $t+t'$

- temporal Wigner transformation:

$$\rho(t, t', |\mathbf{p}|) \;\rightarrow\; \rho(X^0, \omega, |\mathbf{p}|)$$

center-of-mass time $X^0 = \frac{t+t'}{2}$

frequency

The two-point functions become time-translation invariant.

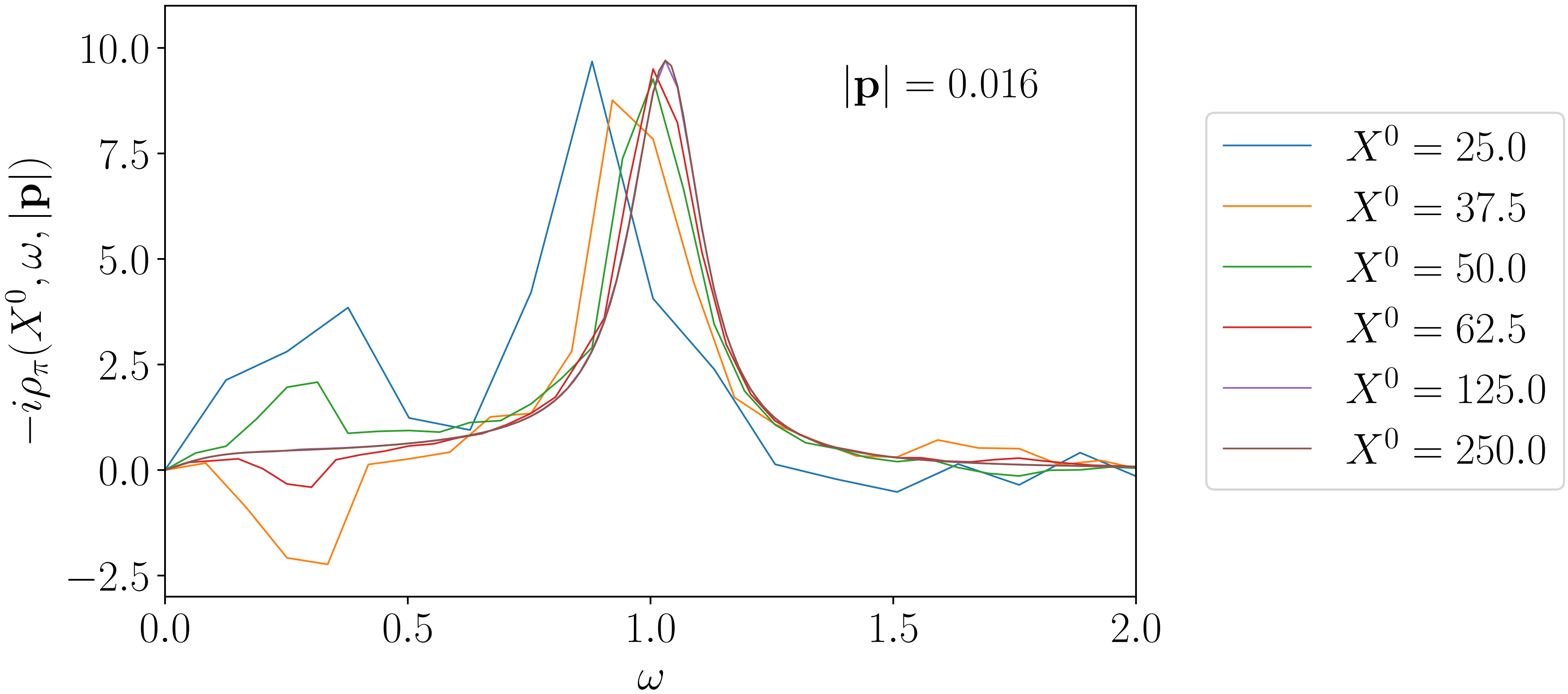

The two-point functions become time-translation invariant.

constant in $X^0 \sim t + t'$ for $X^0 \gtrsim 150$

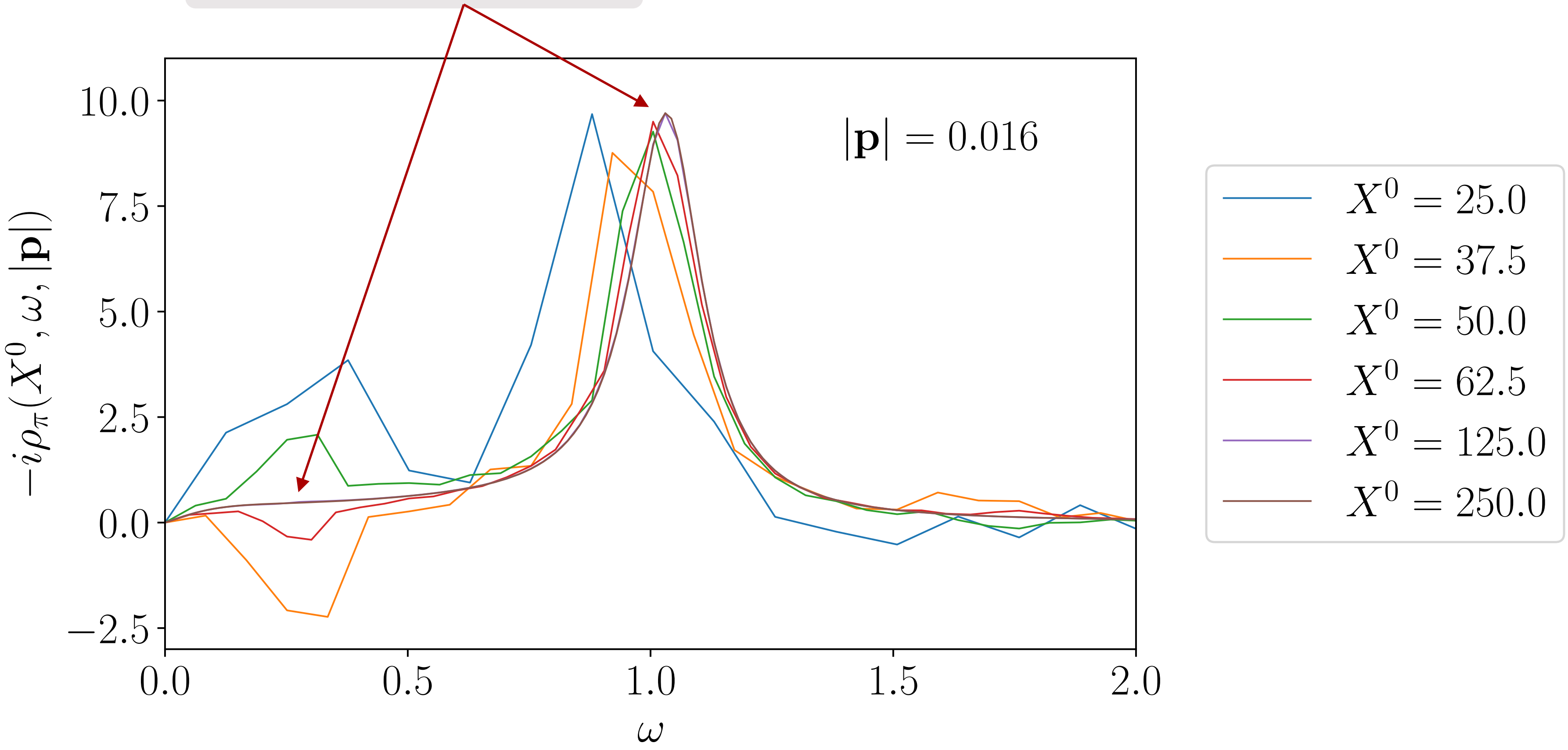

(2) Thermal eq. as state with thermal particle distributions.

- thermal initial density matrix implies fluctuation-dissipation relation:

$$F_{\text{eq}}(\omega, |\mathbf{p}|) = -i\left(\frac{1}{2} + n_{\text{th}}(\omega)\right)\rho_{\text{eq}}(\omega, |\mathbf{p}|)$$

- effective particle number:

$$n(\omega, |\mathbf{p}|) = i\,\frac{F(\omega, |\mathbf{p}|)}{\rho(\omega, |\mathbf{p}|)} - \frac{1}{2}$$

- in thermal equilibrium:

$$n(\omega, |\mathbf{p}|) \to n_{\mathrm{BE/FD}}(\omega) = \frac{1}{e^{\beta\omega} \mp 1} \text{ with } \beta = 1/T$$

Determination of the thermalization temperature using the Bose-Einstein and Fermi-Dirac distribution

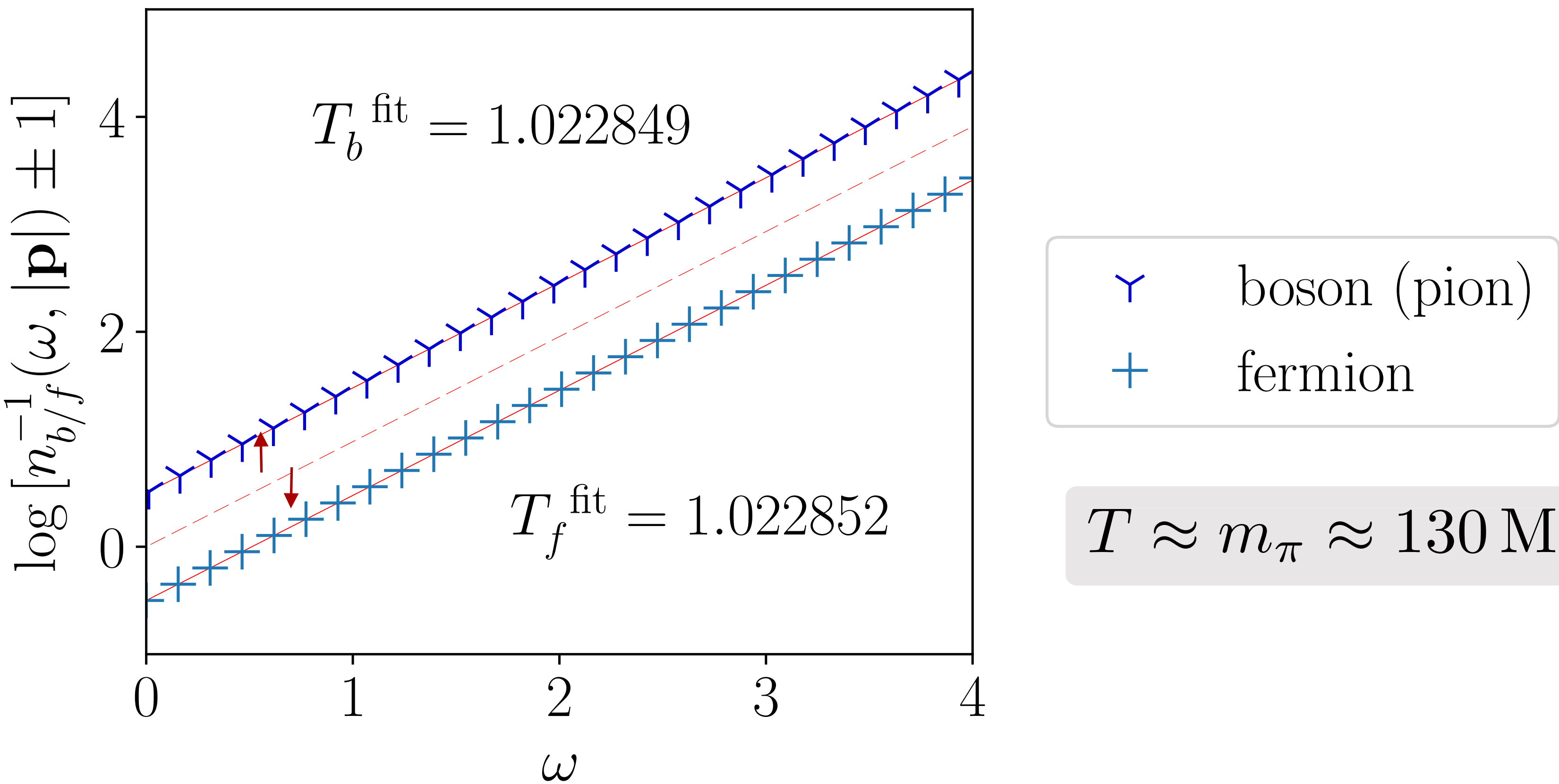

$$T \approx m_\pi \approx 130\,\mathrm{MeV}$$

Particle masses from spectral functions by dispersion relation

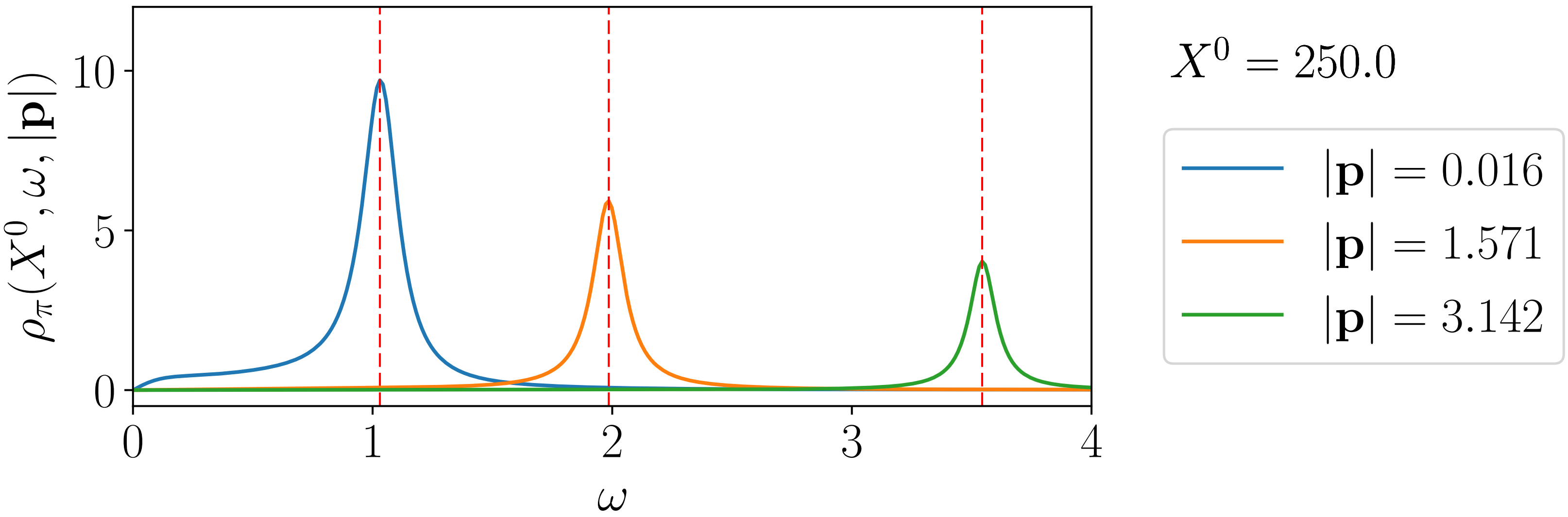

- particle mass from peak position:

$$m(|\mathbf{p}|) = \sqrt{\omega^2_{\text{peak}}(|\mathbf{p}|^2) - |\mathbf{p}|^2}$$

- physical mass at zero momentum

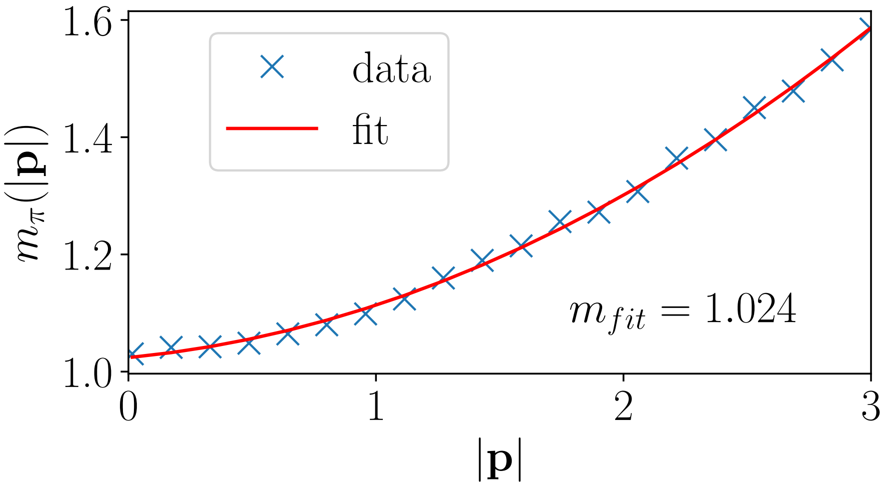

Particle masses from spectral functions: Breit-Wigner fit

$$\rho_{\text{fit}}(\omega) = \frac{2\omega\Gamma}{[\omega^2 - m^2]^2 + \omega^2\Gamma^2} + \delta\, \frac{2\Gamma^2}{[\omega^2 - m^2]^2 + \omega^2\Gamma^2},$$

mass of particle

skewness parameter

width

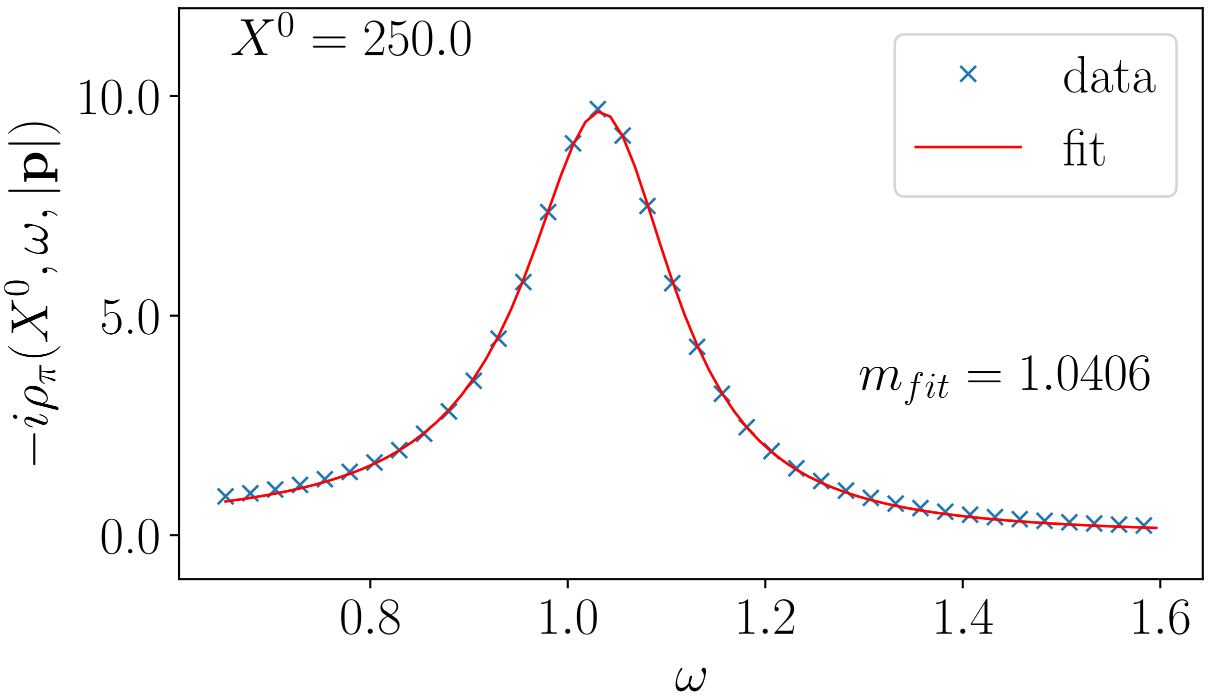

Results in MeV converted by using $m_\pi = 135\,\mathrm{MeV}$

m_ψ^{bare}	13,00	23,40	52,00
m_σ	241,65	228,15	211,95
m_q	205,20	191,70	184,95
f_π	91,80	82,35	71,55
T_{th}	148,50	133,65	118,80

A step forward
in describing the thermalizing of the QGP in a heavy ion collision

We were able to

- include non-equilibrium dynamics
- observe the approach of thermal equilibrium
- determine the physical mass spectrum

Next steps:

- non-zero baryon-chemical potential
- expanding box size
- scaling behavior around critical point

Phase diagram of the quark-meson model

The quark-meson model provides a successful formulation of QCD below scales ~1 GeV.

$$S[\bar{\psi},\psi,\sigma,\pi] = \int_x \Big[\bar{\psi}\left[i\gamma^\mu\partial_\mu - \cancel{m_\psi}\right]\psi - \frac{g}{N_f}\bar{\psi}\left[\sigma + i\gamma_5\tau^\alpha\pi^\alpha\right]\psi$$

$$+\frac{1}{2}\left[\partial_\mu\sigma\partial^\mu\sigma + \partial_\mu\pi^\alpha\partial^\mu\pi^\alpha\right] - \frac{1}{2}m^2\left[\sigma^2 + \pi^\alpha\pi^\alpha\right] - \frac{\lambda}{4!N}\left[\sigma^2+\pi^\alpha\pi^\alpha\right]^2 \Big]$$

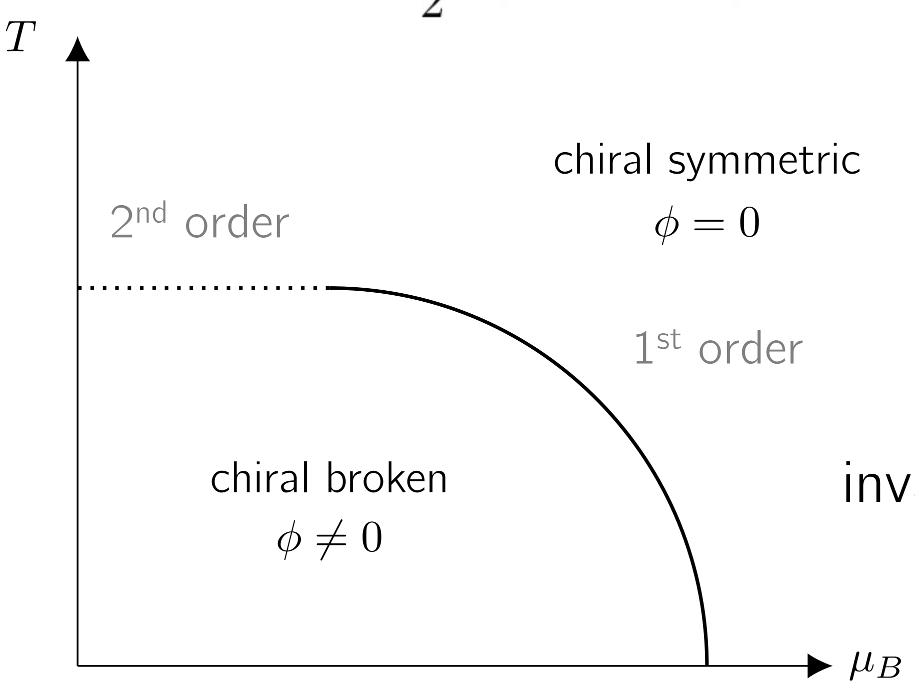

invariance under chiral transformations

$$SU(2)_L \times SU(2)_R \sim O(4)$$

The quark-meson model provides a successful formulation of QCD below scales ~1 GeV.

$$S[\bar{\psi},\psi,\sigma,\pi] = \int_x \Big[\bar{\psi}\,[i\gamma^\mu \partial_\mu - m_\psi]\,\psi - \frac{g}{N_f}\bar{\psi}\,[\sigma + i\gamma_5 \tau^\alpha \pi^\alpha]\,\psi$$

$$+ \frac{1}{2}\,[\partial_\mu \sigma \partial^\mu \sigma + \partial_\mu \pi^\alpha \partial^\mu \pi^\alpha] - \frac{1}{2} m^2\,[\sigma^2 + \pi^\alpha \pi^\alpha] - \frac{\lambda}{4!N}\,[\sigma^2 + \pi^\alpha \pi^\alpha]^2 \Big]$$

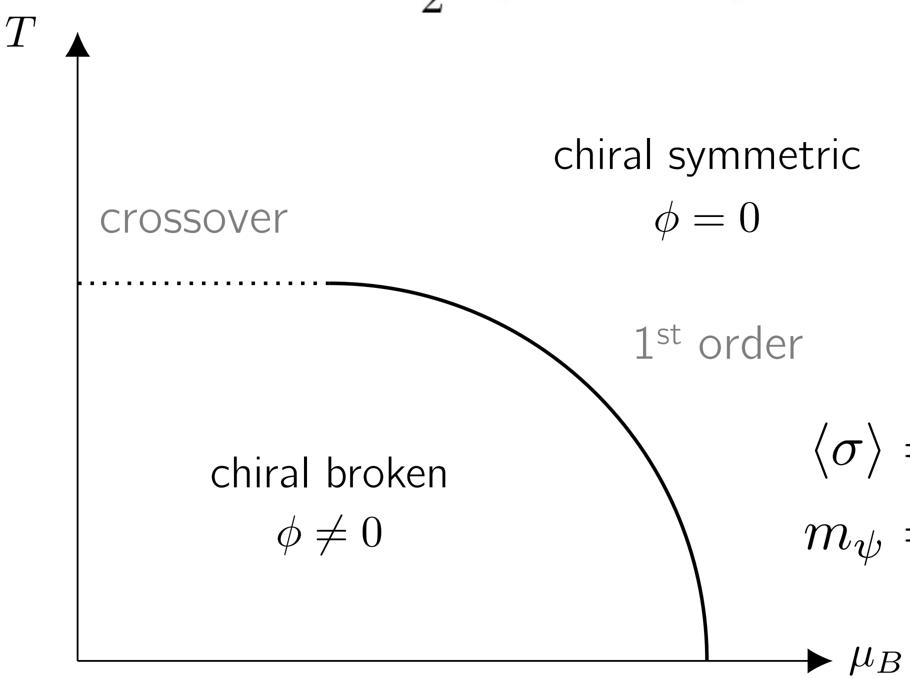

$\langle \sigma \rangle \neq 0$: spontaneous symmetry breaking

$m_\psi \neq 0$: explicit symmetry breaking

Wigner transformation

Computation of spectral functions in spatial Fourier and temporal Wigner space

- Definition of the temporal Wigner transformation:

$$\rho(X^0,\omega,|\mathbf{p}|) = \int_{-2X^0}^{2X^0} \mathrm{d}s\; e^{i\omega s}\rho\left(X^0+\frac{s}{2}, X^0-\frac{s}{2}, |\mathbf{p}|\right)$$

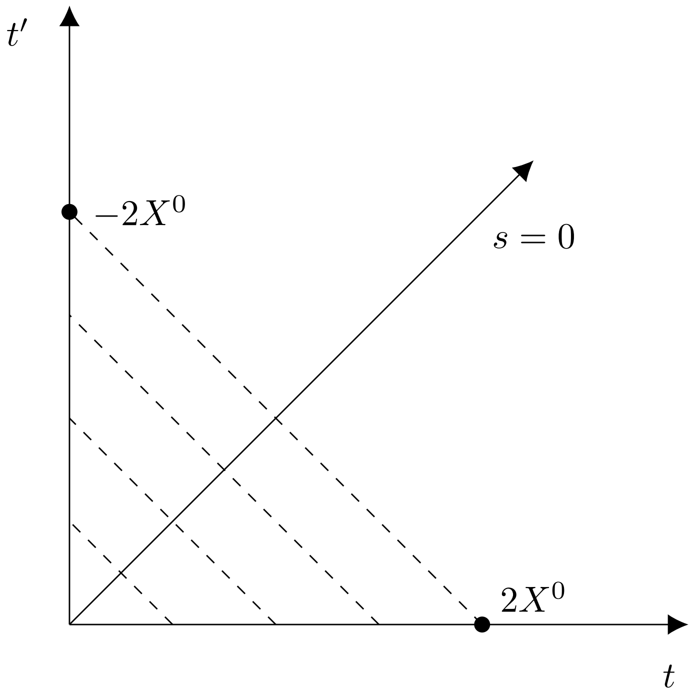

with relative time $s = t - t'$,

center-of-mass time $X^0 = \dfrac{t+t'}{2}$

$$\boxed{\rho(t,t',|\mathbf{p}|) \;\rightarrow\; \rho(X^0,\omega,|\mathbf{p}|)}$$

spectral function in terms of center-of-mass time and frequency

2PI effective action techniques

Schwinger-Keldysh contour for initial value problems

- expectation value:

$$\langle \mathcal{O}(t) \rangle = \frac{\mathrm{Tr}[\rho(t)\mathcal{O}]}{\mathrm{Tr}[\rho(t)]}$$

von Neumann equation

$$\text{with } \rho(t) = U_{t,t_0}\rho(t_0)U_{t_0,t}$$

- only need initial density matrix:

$$\langle \mathcal{O}(t) \rangle = \frac{\mathrm{Tr}\big[\rho(t_0)\; U_{t_0,t}\mathcal{O}U_{t,t_0}\big]}{\mathrm{Tr}\big[\rho(t_0)\big]}$$

Schwinger-Keldysh contour

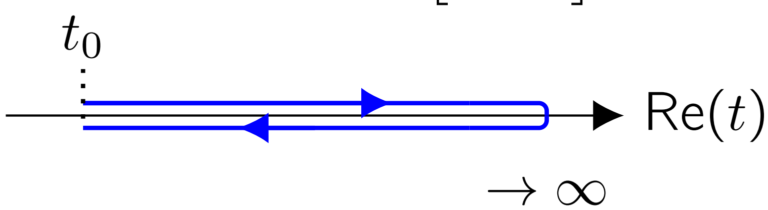

- generating functional:

$$Z[J,R;\rho] = \mathrm{Tr}\Big[\rho(t_0)\; T_{\mathcal{C}}\; e^{iJ\cdot\varphi + \frac{i}{2}\varphi\cdot R\cdot\varphi}\Big]$$

source terms

Initial conditions

$$Z[J,R;\rho] = \mathsf{Tr}\left[\rho(t_0)\ T_{\mathcal{C}}\ e^{iJ\cdot\varphi+\frac{i}{2}\varphi\cdot R\cdot\varphi}\right]$$

in equilibrium

$$\rho^{\mathrm{th}} \sim e^{-\beta H} \sim U_{t_0-i\beta,t_0}$$

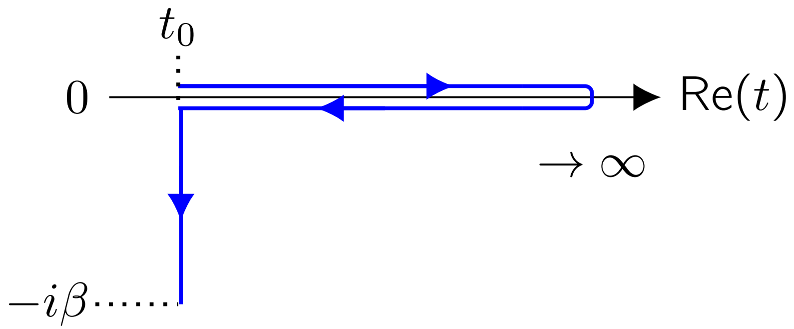

Initial conditions

$$Z[J,R;\rho] = \mathrm{Tr}\Big[\rho(t_0)\; T_{\mathcal{C}}\; e^{iJ\cdot\varphi+\frac{i}{2}\varphi\cdot R\cdot\varphi}\Big]$$

in equilibrium

$$\rho^{\mathrm{th}} \sim e^{-\beta H} \sim U_{t_0-i\beta,t_0}$$

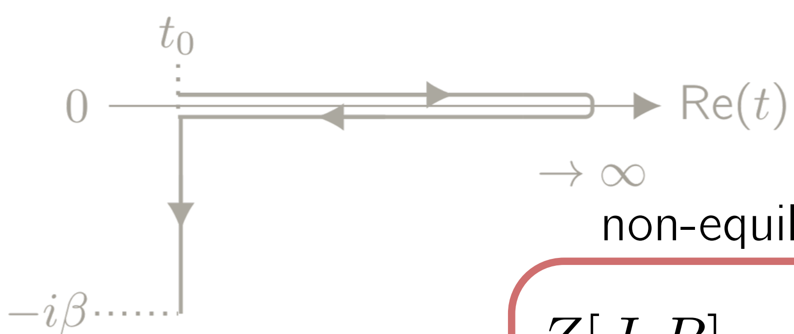

out of equilibrium

$$\rho^{\text{Gauss}} \sim e^{ia\cdot\varphi+i\varphi\cdot b\cdot\varphi}$$

non-equilibrium generating functional for $\rho^{\text{Gauss}}(t_0)$

$$Z[J,R] = e^{iW[J,R]} = \int \mathcal{D}\varphi\; e^{iS[\varphi]+iJ\cdot\varphi+\frac{i}{2}\varphi\cdot R\cdot\varphi}$$

with 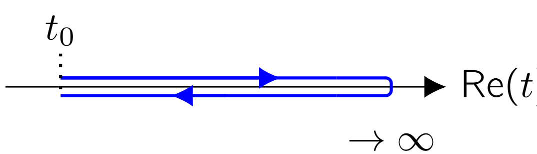

classical action
$S[\varphi]$

generating functional with 2 source terms:

$$Z[J,R] = e^{iW[J,R]} = \int \mathcal{D}\varphi \; e^{iS[\varphi] + iJ\cdot\varphi + \frac{i}{2}\varphi\cdot R\cdot\varphi}$$

one-point function
(macroscopic field)

$$\phi(x) = \frac{\delta W[J,R]}{\delta J(x)}$$

two-point function
(propagator)

$$G(x,y) = \frac{\delta W[J,R]}{\delta R(x,y)} - \frac{1}{2}\phi(x)\phi(y)$$

2PI effective action
$\Gamma[\phi, G]$

$$= W - \frac{\delta W}{\delta J}\cdot J - \frac{\delta W}{\delta R}\cdot R$$

double Legendre
transformation

2PI effective action $\Gamma[\phi, G, \Delta]$ $= S[\phi] +$ 1-loop quantum corrections $+$ 2PI diagrams

$$\overbrace{\underbrace{\text{LO diagrams}}_{\sim N^1} + \underbrace{\text{NLO diagrams}}_{\sim N^0} + \underbrace{\text{NNLO diagrams}}_{\sim N^{-1}} + \dots}^{\text{large } N \text{ expansion for bosons}} + \text{fermion-boson-loop}$$

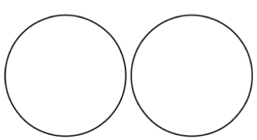

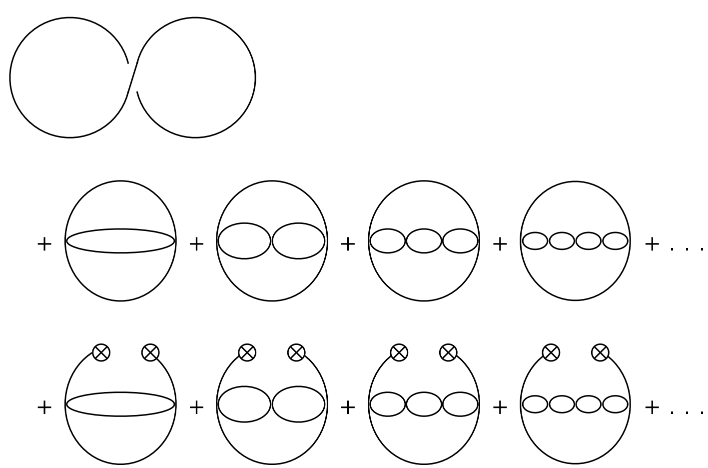

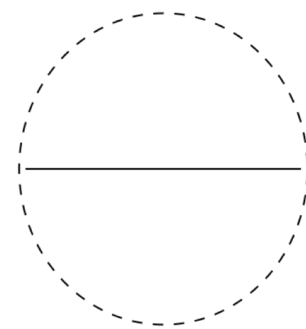

no further fermion contributions due to low occupation number

$$\underbrace{\boxed{\text{2PI effective action } \Gamma[\phi, G, \Delta]} = S[\phi] + \text{1-loop quantum corrections}}_{} + \text{2PI diagrams}$$

$$\Gamma[\phi, G, \Delta] = S[\phi] + \frac{i}{2}\mathrm{Tr}\ \ln\left[G^{-1}\right] + \frac{i}{2}\mathrm{Tr}\ \left[G_{\mathrm{cl}}^{-1}(\phi)G\right]$$

$$- i\mathrm{Tr}\ \ln\ \left[\Delta^{-1}\right] - i\mathrm{Tr}\ \left[\Delta_{\mathrm{cl}}^{-1}(\phi)\Delta\right]$$

2PI effective action
$\Gamma[\phi, G]$

stationary conditions:

$$\left.\frac{\delta\Gamma[\phi,G]}{\delta\phi(x)}\right|_{\phi=\bar{\phi},G=\bar{G}(\phi)} = 0, \qquad \left.\frac{\delta\Gamma[\phi,G]}{\delta G(x,y)}\right|_{\phi,G=\bar{G}(\phi)} = 0$$

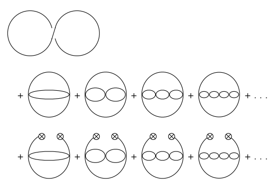

$$i\bar{G}^{-1}(x,y;\phi) = iG_{\text{cl}}^{-1}(x,y;\phi) - i\Sigma(x,y;\phi,G)\Big|_{G=\bar{G}(\phi)}$$

classical propagator   self-energy

evolution equations
for ϕ and G

$$\left[\partial_t^2 + M^2(x;\phi)\right]\phi(t) = \text{fermion backreaction + 2PI corrections}$$

$$\left[\Box_x + M^2(x;\phi)\right]G(x,y) = -i\int_z \left[\Sigma(x,z;\phi,G)\right]G(z,y) - i\delta(x-y)$$

effective mass

evolution equations for ϕ, G, Δ

- Spatial homogeneity and isotropy

$$G(x,y) \to G(t,t',|\mathbf{p}|)$$

- Boson sector: $\langle\sigma\rangle \neq 0,\ \langle\pi\rangle = 0$

$$G \to \text{longitudinal } (\sigma) + \text{transverse } (\pi) \text{ direction}$$

- Fermion sector:

$$\Delta \to \text{Lorentz components } S, 0, V, T$$

- Propagator decomposition:

$$G(x,y) = F(x,y) + \frac{i}{2}\rho(x,y)\,\mathrm{sgn}(x^0 - y^0)$$

statistical function

spectral function

evolution equations for ϕ, G, Δ

coupled integro-differential equations for

$F_\sigma^\phi(x^0, y^0, \lvert\mathbf{p}\rvert),\ F_\pi^\phi(x^0, y^0, \lvert\mathbf{p}\rvert)$	real, symmetric
$\rho_\sigma^\phi(x^0, y^0, \lvert\mathbf{p}\rvert),\ \rho_\pi^\phi(x^0, y^0, \lvert\mathbf{p}\rvert)$	real, antisymmetric
$F_S^\psi(x^0, y^0, \lvert\mathbf{p}\rvert),\ F_V^\psi(x^0, y^0, \lvert\mathbf{p}\rvert),\ F_T^\psi(x^0, y^0, \lvert\mathbf{p}\rvert)$	real, symmetric
$\rho_S^\psi(x^0, y^0, \lvert\mathbf{p}\rvert),\ \rho_V^\psi(x^0, y^0, \lvert\mathbf{p}\rvert),\ \rho_T^\psi(x^0, y^0, \lvert\mathbf{p}\rvert)$	real, antisymmetric
$F_0^\psi(x^0, y^0, \lvert\mathbf{p}\rvert)$	imaginary, antisymmetric
$\rho_0^\psi(x^0, y^0, \lvert\mathbf{p}\rvert)$	imaginary, symmetric

$$\sigma(t)$$

evolution equations for ϕ, G, Δ

coupled integro-differential equations like

$$\left[\partial_t^2 + |\mathbf{p}|^2 + M_\sigma^2(t)\right] F_\sigma(t,t',|\mathbf{p}|) = -\int_{t_0}^{t} \mathrm{d}t'' A_\sigma(t,t'',|\mathbf{p}|)F_\sigma(t'',t',|\mathbf{p}|) + \int_{t_0}^{t'} \mathrm{d}t'' C_\sigma(t,t'',|\mathbf{p}|)\rho_\sigma(t'',t',|\mathbf{p}|)$$

$$\begin{aligned} i\partial_t F_S(t,t',|\mathbf{p}|) = & -i|\mathbf{p}|\; F_T(t,t',|\mathbf{p}|) + M_\psi(t)F_0(t,t',|\mathbf{p}|) \\ & + \int_{t_0}^{t} \mathrm{d}t'' \Big[A_S(t,t'',|\mathbf{p}|)\; F_0(t'',t',|\mathbf{p}|) + A_0(t,t'',|\mathbf{p}|)\; F_S(t'',t',|\mathbf{p}|) \\ & \qquad + iA_V(t,t'',|\mathbf{p}|)\; F_T(t'',t',|\mathbf{p}|) - iA_T(t,t'',|\mathbf{p}|)\; F_V(t'',t',|\mathbf{p}|)\Big] \\ & + \int_{t_0}^{t'} \mathrm{d}t'' \Big[-C_S(t,t'',|\mathbf{p}|)\; \rho_0(t'',t',|\mathbf{p}|) - C_0(t,t'',|\mathbf{p}|)\; \rho_S(t'',t',|\mathbf{p}|) \\ & \qquad - iC_V(t,t'',|\mathbf{p}|)\; \rho_T(t'',t',|\mathbf{p}|) + iC_T(t,t'',|\mathbf{p}|)\; \rho_V(t'',t',|\mathbf{p}|)\Big], \end{aligned}$$

Discretized evolution equations

$$\rho_\sigma(i+1,j) = 2\rho_\sigma(i,j) - \rho_\sigma(i-1,j) - dt^2\Big[|\mathbf{p}|^2 + M^2{}_\sigma(t)\Big]\rho_\sigma(i,j)$$
$$- dt^3\left[\frac{1}{2}A_\sigma(i,i)\rho_\sigma(i,j) + \sum_{l=i+1}^{j-1} A_\sigma(i,l)\rho_\sigma(l,j) + \frac{1}{2}A_\sigma(i,j)\rho_\sigma(j,j)\right]$$

$$\rho_T(i+1,j) = \rho_T(i-1,j) + 2\ dt\Big[|\mathbf{p}|\rho_S(i,j) - M_\psi(t)\rho_V(i,j)\Big]$$
$$- 4\ dt^2\left[\frac{1}{2}A_S(i,i)\rho_V(i,j) + \sum_{l=i+1}^{j-1} A_S(i,l)\rho_V(l,j) + \frac{1}{2}A_S(i,j)\rho_V(j,j) + \ \ldots\right]$$

Numerical Set-up

Quench in the 1st time step

initial conditions:
propagators of the free theory,
zero macroscopic field

non-equilibrium time-evolution:
Mexican hat potential allowing
for spontaneous symmetry
breaking

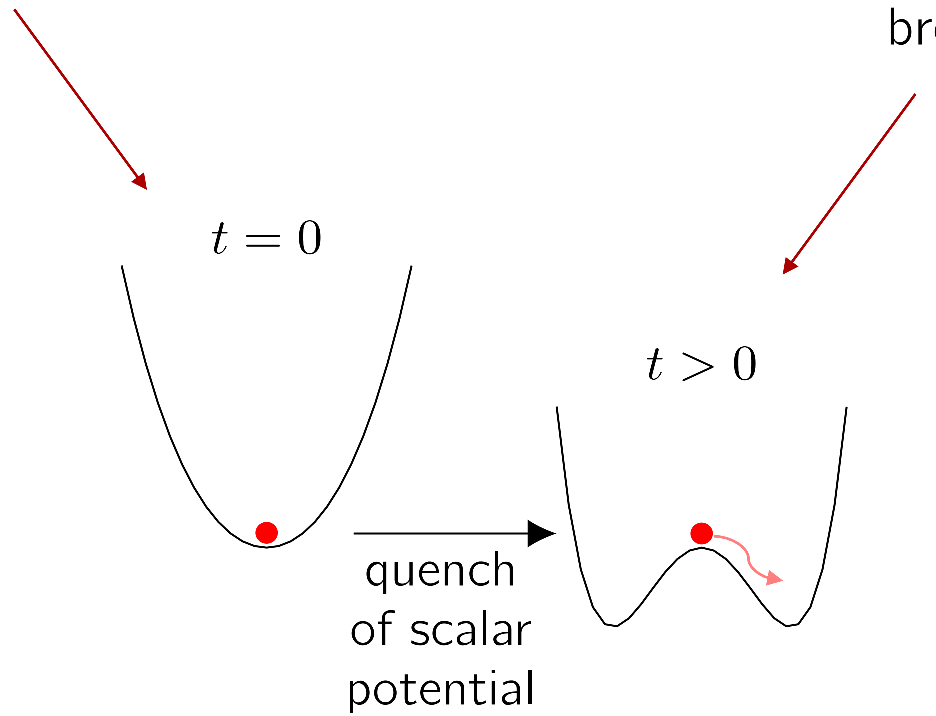

Input parameters

parameter	value
λ	90.0
m^2	-0.008
m_ψ	0.18
g	5.0

$$dx = 0.2$$
$$N_x = 200$$
$$dt = 0.01$$
$$N_t = 5000$$

Input parameters in MeV converted by using $m_\pi = 135\,\mathrm{MeV}$

Parameter	Value in MeV
λ	90,0
m^2	-23,3
m_ψ	23,4
g	5,0

Numerical Results

Bose-Einstein distribution

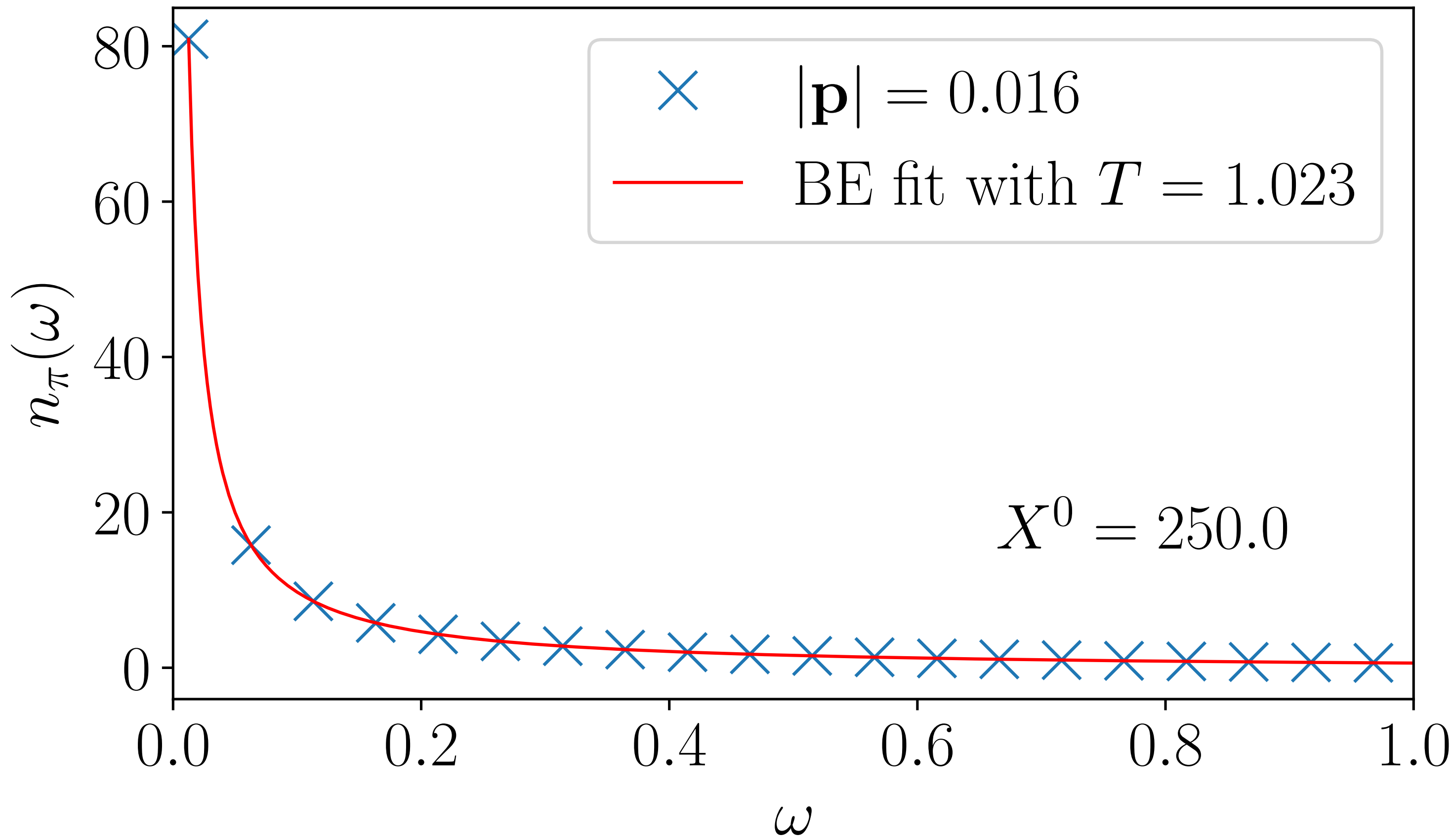

Particle masses from spectral functions: Breit-Wigner fit

$$\rho_{\text{fit}}(\omega) = \frac{2\omega\Gamma}{\left[\omega^2 - m^2\right]^2 + \omega^2\Gamma^2} + \delta \, \frac{2\Gamma^2}{\left[\omega^2 - m^2\right]^2 + \omega^2\Gamma^2},$$

mass of particle

skewness parameter

width

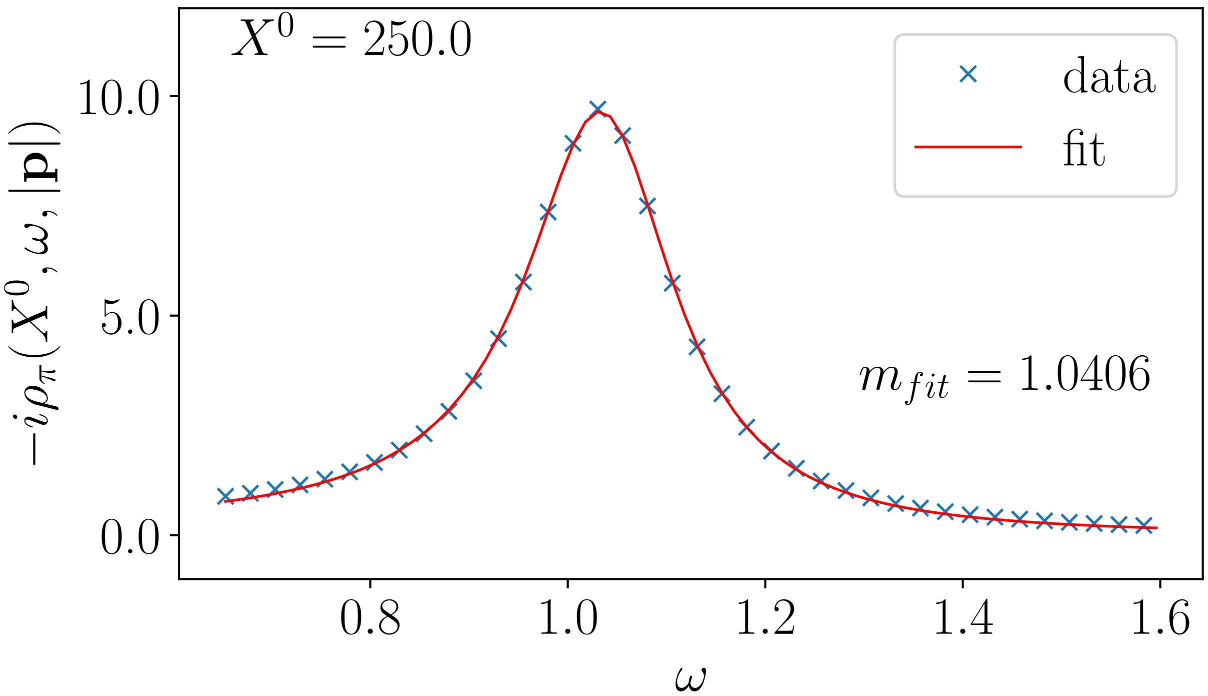

Results in MeV converted by using $m_\pi = 135\,\mathrm{MeV}$

m_ψ^{bare}	13,00	23,40	52,00
m_σ	241,65	228,15	211,95
m_q	205,20	191,70	184,95
f_π	91,80	82,35	71,55
T_{th}	148,50	133,65	118,80